Int. J. Electrochem. Sci., 13 **(2018)** 8633 – 8644, doi: 10.20964/2018.09.08

International Journal of ELECTROCHEMICAL SCIENCE
www.electrochemsci.org

Short Communication

Enzyme-Free Glucose Sensor Based on Micro-nano Dualporous Gold-Modified Screen-Printed Carbon Electrode

Nguyen Xuan Viet[1,2], *Miyuki Chikae*[1], *Yoshiaki Ukita*[1], *and Yuzuru Takamura*[1]

[1] School of Materials Science, Japan Advanced Institute of Science and Technology (JAIST), 1-1 Asahidai, Nomi City, Ishikawa 923-1292, Japan.
[2] Faculty of Chemistry, VNU University of Science, Vietnam National University, Hanoi, 19 Le Thanh Tong, Hoan Kiem District, Ha Noi, Vietnam.
[*]E-mail: vietnx@vnu.edu.vn

Received: 18 December 2017 / *Accepted:* 28 June 2018 / *Published:* 5 August 2018

In this work, an enzyme-free glucose sensor at neutral pH (7.4) has been developed based on a micro-nano dualporous (MNDP) gold-modified screen-printed carbon electrode (SPCE). The combination of MNDP gold and SPCE makes the device a compact, low-cost and reliable enzyme-free glucose sensor. MNDP gold was directly synthesized via an electrochemical deposition method on a carbon surface using a hydrogen bubble as a dynamic template. The obtained MNDP gold has a highly porous structure and is mechanically stable. The MNDP gold-modified SPCE was applied to glucose sensing. This enzyme-free sensor showed a wide linear range, with the logarithm of glucose concentration between 1.5 and 16 mM, a high sensitivity of 48.4 $\mu A.mM^{-1}.cm^{-2}$, and a limit of detection of 25 µM. It also exhibited exquisite selectivity with the common interference compounds in real samples. Moreover, this sensor successfully detects glucose levels in human blood serum with satisfactory results and functional recovery.

Keywords: Enzyme-Free, Glucose Sensor, Screen-Printed Carbon Electrode, Micro-Nano Dualporous Gold.

1. INTRODUCTION

Accurate, rapid, selective, inexpensive and stable sensors for monitoring glucose levels in human blood or serum are currently necessary for the diagnosis and management of diabetes mellitus [1]. Most well-known biosensors for detecting glucose concentration are based on the following: immobilized glucose oxidase or glucose dehydrogenase, electrochemical detection of enzymatically generated hydrogen peroxide, or redox mediators, such as derivatives of ferrocene, ferro/ferricyanide, hydroquinone and other redox organic dyes [2, 3]. Although enzymatic glucose sensors usually exhibit high selectivity and good sensitivity, the main drawback of these sensors is the natural instability of the

immobilized enzyme with temperature, pH, humidity, and ionic detergents, leading to lack of stability and accuracy during storage and use [4-6]. The detection of enzymatically liberated hydrogen peroxide usually needs a high overpotential and is less accurate due to the combined presence of other redox-active molecules, such as ascorbic acid (AA) and uric acid (UA), in biological fluids [7]. Many studies have attempted to overcome these difficulties with various materials.

An enzyme-free glucose sensor, the next generation of glucose sensors, possesses advantages over enzymatic glucose sensors, such as stability, simplicity, reproducibility and freedom from oxygen limitation [8]. These sensors are expected to overcome problems for practical uses based on the direct oxidation of glucose on the electrode surface without the use of a fragile enzyme [9]. These sensors are modified with nanomaterials, such as nanostructured Pt [10], Au [11], Pd [12], Cu_xO [13, 14], Ni [15, 16], nanowires [17], nanoparticle modified carbon nanotubes [18] and porous nanomaterials [19-21]. Specifically, porous materials with a high surface area, large pore volume, and stably tailored components have received much attention because of their wide application as absorbents, catalysts and thermal insulators [22]. Porous materials have been synthesized by various methods, such as dealloying [19], template electrochemical deposition [23], self-assembly [7] and dynamic bubble template electrochemical deposition [24, 25]. With the advantages of requiring less time, simplicity, being green, and not requiring a post-synthesis process, bubble dynamic template electrochemical deposition is beneficial as a simpler and quicker process to synthesize porous structures to apply to an enzyme-free glucose sensor. Among nanostructured materials, gold is an attractive metal because gold electrodes present higher activity and less overpotential for oxidation in neutral and alkaline media compared with other metals [26, 27].

The screen-printed carbon electrode (SPCE), a disposable three-electrode system, was successfully produced in our laboratory with the advantage of fabricating a large number of near-identical electrodes at a low cost [28]. SPCE is printed on insulator substrates as a plastic or ceramic. Difference between other materials, such as Cu, Au, Pt, and stainless steel, used as electrode substrates creates challenges in experimental setup and is non-user friendly in practical application. The SPCE is a compact three-electrode system that is disposable and easy to modify. It has been successfully applied to fabricate biosensors and immunosensors in our group [28-31]. Thus, SPCE may become a reliable solution for enzyme-free glucose sensors in practical use.

In this work, we report the fabrication of a simple enzyme-free electrode based on MNDP gold-modified SPCE. In this way, a highly stable, fast and disposable sensor was fabricated for the highly sensitive amperometric detection of glucose. This enzyme-free glucose sensor is also compact compared with previous sensors, which required an alkaline medium or were constructed on gold or platinum surfaces. Thus, these previous sensors possessed complicated measurement setups that limit their application to practical uses.

2. EXPERIMENTAL

2.1. Reagents

$HAuCl_4$, D-glucose and ascorbic acid were purchased from Sigma-Aldrich (Japan). $NaH_2PO_4 \cdot 2H_2O$, Na_2HPO_4, NaCl, and KH_2PO_4 were purchased from Wako Pure Chemical Industries

(Osaka, Japan). SPCE with a working electrode area of 2.64 mm^2 was purchased from Biodevice Technology (Ishikawa, Japan). Other reagents were of analytical grade, and all solutions were prepared and diluted using ultra-pure water (18.2 MΩ.cm) from the Milli-Q system (Millipore, Billerica, MA, USA).

2.2. Instruments

Scanning electron microscopy (SEM) images were observed using a Hitachi S-4100 with an accelerating voltage of 20 kV. Electrochemical measurements were taken on an ALS/CH Instruments electrochemical analyzer, model 730C (Austin, TX, USA). A drop of 35 µL of the electrolyte solution was applied to the three electrodes of SPCE. BT 3000Plus for clinical chemistry (Biotecnica Instruments - Italia) was used to analyze the glucose content in human serum samples for comparison. All experiments were performed at room temperature (25 °C).

2.3. Synthesis of MNDP gold-modified SPCE and glucose measurements

MNDP gold was electrodeposited on SPCE (figure 1a) with a hydrogen bubble as a dynamic template from a drop (35 µL) of solution containing 5 mM $HAuCl_4$ by modification of previously reported procedures [25, 32]. The current density was controlled as high as 3 $A.cm^{-2}$ for 100 s at room temperature. After the electrodepositing process, the MNDP gold-modified SPCE electrode was washed three times with pure water and blown dry under a stream of N_2 gas. The electrodes were then kept in a box at room temperature until use. Gold nanoparticle-modified SPCEs were electrodeposited using a cyclic voltammetry technique in 5 mM $HAuCl_4$ solution, similar to the previously reported procedure [33]. Briefly, CV was swept from -0.7 V to 0.4 V vs. AgCl/Ag for 10 cycles at a scan rate of 50 mV/s. Then, the modified SPCE was washed with pure water and dried naturally at room temperature.

Electrochemical measurements to characterize the electrochemical behavior of electrodes were performed on a three-electrode system, in which carbon was the counter, AgCl/Ag was the reference and MNDP gold was the working electrode. Phosphate buffered saline (PBS, 0.1 M) was used during all electrochemical measurements. Prepared D-glucose solutions were allowed to stand overnight at room temperature before electrochemical measurement. Cyclic voltammetry was swept from -1.0 to 0.6 V vs. AgCl/Ag at scan rate of 20 mV/s. Amperometry was conducted at the optimized potential of the glucose sensor in a constantly stirred (500 rpm) PBS solution; then, a certain amount of stock glucose solution (0.1 M) was added to increase the glucose concentration.

3. RESULTS AND DISCUSSION

3.1. Synthesis and characterization of MNDP gold

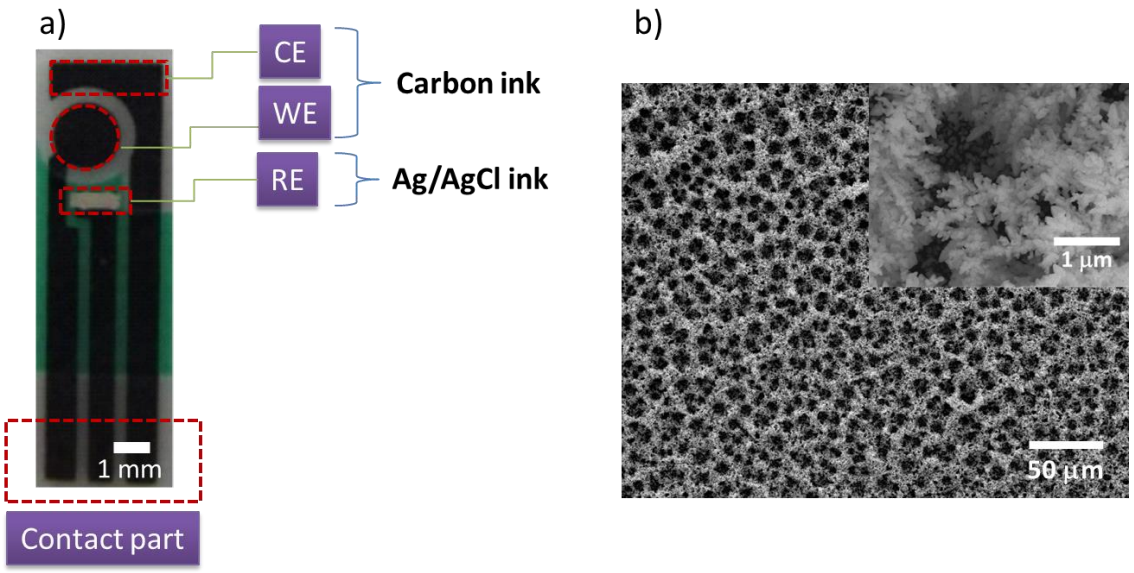

Figure 1. a) Photo of the screen-printed carbon electrode (SPCE) used in this enzyme-free glucose sensor. b) SEM images of electrodeposited MNDP gold observed on the surface of the screen-printed carbon electrode, inset: high magnification of MNDP gold.

It was thought that the synthesis of gold foams by electrochemical deposition was a challenge due to the low overpotential of hydrogen evolution on the substrate material [34]. However, S. Cherevko et al. showed the successful synthesis of nanopore-containing gold foam with a multi-porous size distribution on a Pt/Ti/Si substrate via electrochemical deposition [32]. The successfully synthesized nanoporous gold was achieved by adding NH_4^+ containing salt to the electrolysis solution. In our case, the MNDP gold layer was synthesized successfully and rapidly by taking advantage of a hydrogen bubble as the dynamic template during the electrodepositing process on the surface of a carbon material, which usually has high overpotential with hydrogen. The typical morphology of the electrodeposited MNDP gold on the carbon substrate observed by SEM is shown in **Error! Reference source not found.**b. It can be seen that the walls of the structure are included in numerous ramified deposits that constitute many nanoparticles. This electrodeposited gold structure is similar to previously reported structures [32, 34]. The porosity and grain size of MNDP gold is estimated to be approximately 10 µm and 100 nm from the SEM images, respectively. The surface area of MNDP gold-modified SPCE was ~50 times higher than that of SPCE. This increase was estimated using cyclic voltammetry in 0.5 M H_2SO_4 solution [8, 23]. Direct electrochemical deposition of MNDP gold also exhibits some advantages, such as a short preparation time, a lack of post-deposition treatment, being green and having well-defined geometry, over other methods for synthesizing porous materials (see table 1) [35-38].

3.2. Electrochemical oxidation of glucose

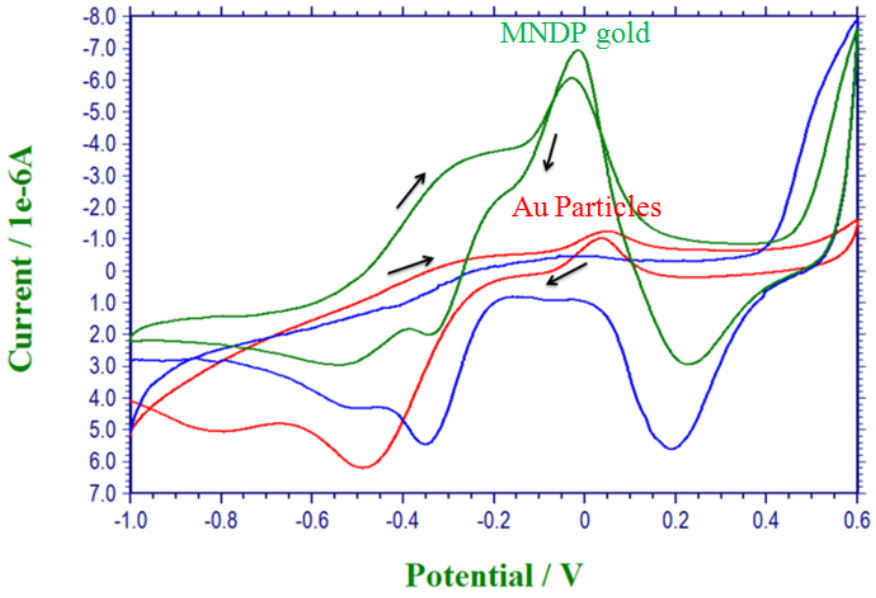

Figure 2. Typical CVs of MNDP gold-modified SPCE in PBS solution (0.1 M, pH 7.4) without glucose (blue) and with 5 mM glucose (green). CV of gold nanoparticle-modified SPCE in PBS solution (0.1 M) with 5 mM glucose (red). Scan rates were 20 mV/s.

1 The electrochemical behavior of the electrodes was studied by cyclic voltammetry.
2

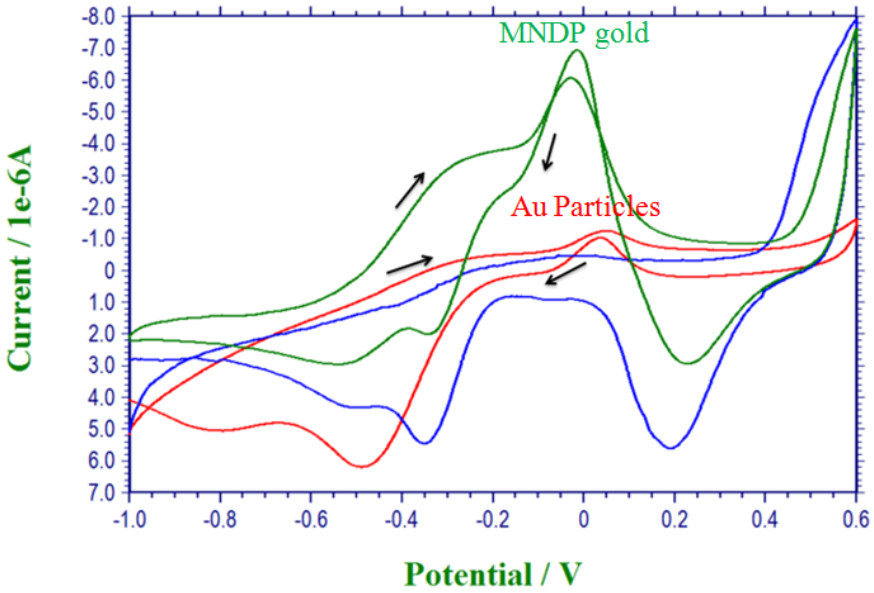

Figure 2 compares the typical cyclic voltammogram (CV) obtained from the electrochemical oxidation of glucose at the MNDP gold-modified SPCE, and gold nanoparticle-modified SPCE electrodes in 0.1 M PBS solution. Without the presence of glucose, the MNDP gold-modified SPCE (blue) shows two peaks on the forward and backward CV located at 0.6 V vs. AgCl/Ag and 0.2 V vs. AgCl/Ag, corresponding to the oxidation of gold into gold oxide and then reduction to gold again in

0.1 M PBS solution, respectively [20] [26]. Before the oxidation peak, the increase of current intensity in the potential region from approximately -0.4 V to +0.1 V can be attributed the chemisorption of the OH^- anion from H_2O to form $AuOH_{ads}$, a precursor of oxide formation [20, 39].

$$H_2O \rightarrow OH^- + H^+ \quad (1)$$

$$Au + OH^- \rightarrow AuOH_{ads} + e^- \quad (2)$$

When an aliquot of glucose solution was dropped on these modified electrodes, the gold nanoparticle-modified SPCE (red) shows a small current response for the electrochemical oxidation of glucose at potential of ~ +0.04 V vs. AgCl/Ag. The mechanism for the electrochemical oxidation of glucose at gold electrodes is a multistep process. This process is considered as illustrated in Scheme 1. The initiating step mediates the chemisorption of OH^- anions onto the surface of the gold, leading to the formation of hydrous gold oxide (AuOH), which is believed to be the catalytic component of gold electrodes [26]. Because it is accepted that the formation of AuOH sites is the key step for the electrochemical oxidation of glucose, the oxidation of glucose is thus strongly dependent on the amount of generated AuOH sites. At low potentials, the quantity of AuOH sites is limited on the surface of the electrode, as indicated by the small increase in current intensity. Then, one glucose molecule is oxidized by one AuOH site to generate one molecule of gluconolactone, which will hydrolyze to form gluconic acid [23, 39, 40], resulting in an increased voltammetric current. The oxidation of glucose on the surface of gold is shown in equations (3) and (4) [3]:

$$AuOH + e^- + \text{glucose} \rightarrow Au + \text{gluconolactone} \quad (3)$$

$$\text{Gluconolactone} \rightarrow \text{gluconic acid} \quad (4)$$

As a consequence, the MNDP gold-modified SPCE (green) exhibits much higher current intensity for the oxidation of glucose at less positive potential, ~ -0.03 V vs. AgCl/Ag. The shift toward lower overpotential by ~70 mV in the CV curve was evidence of higher electron transfer efficiency and mass transport in MNDP gold than in gold nanoparticle-modified SPCE. The decreased glucose oxidation overpotential could also suggest the effect of increased surface area of MNDP gold compared with bare and gold nanoparticle-modified SPCE. The beginning of glucose oxidation starts much earlier, at ~ -0.4 V vs. AgCl/Ag, exhibiting a complicated glucose oxidation mechanism [9]. These results show that the MNDP gold-modified SPCE more efficiently catalyzes the glucose oxidation process than gold nanoparticle-modified SPCE.

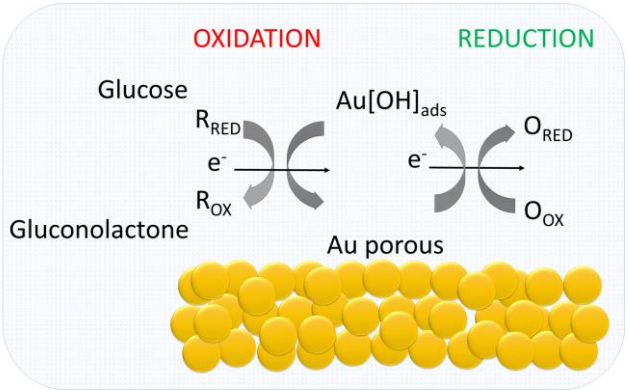

Scheme 1. This scheme exhibits the oxidation process of glucose on MNDP gold in 0.1 M PBS solution during the amperometric measurement.

3.3. Amperometric measurement of glucose

Due to higher sensitivity and simpler practical measurement, amperometry was used to study the response of MNDP gold-modified SPCE to glucose, which is added successively to the electrolyte. Figure 3 shows the typical amperometric response of the MNDP gold-modified SPCE to glucose oxidation in a constantly stirred PBS solution (0.1 M) at an optimized detection potential of -0.2 V vs. AgCl/Ag. A certain amount of stock glucose concentration (0.1 M) was successively added to the electrolyte every 25 s. When an aliquot of glucose solution was added to the stirred PBS solution, the anodic current increased steeply to achieve a new value corresponding to the glucose concentration. The sensor response time reached 95% of the steady-state current within 2.5 s (see the top inset of Figure 3). The response time is comparable with that of porous gold films (2s) [34] and 3D porous Au-Graphene (3s) [41] but is faster than that of 3D nanostructure gold (5s) [20] and porous gold clusters (5s) [42]. The short response time is an indicator of fast charge transport in the MNDP gold layer.

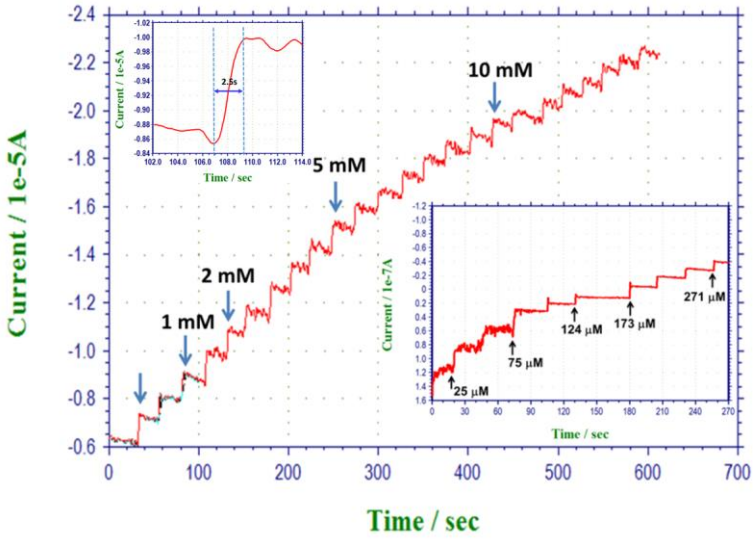

Figure 3. The typical amperometric response of the MNDP gold-modified SPCE to glucose oxidation with successive addition of a certain amount of stock glucose to a stirring 0.1 M PBS solution. The applied potential was -0.20 V vs. AgCl/Ag. The top left inset shows the response time of current when an aliquot of glucose was added to the PBS solution. The bottom right shows the amperometric response of the MNDP gold-modified SPCE to glucose at low concentration.

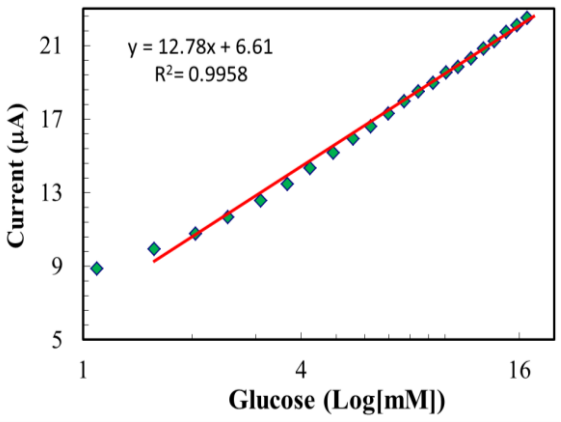

Figure 4. Calibration curve showing the relationship between current intensity (i) vs. Log(C) for the amperometric responses of the MNDP gold-modified SPCE to glucose concentration (0.1 M PBS solution).

The sensor also illustrates the wide dynamic range of glucose concentration, from 25 µM to 16 mM. Figure 4 shows the calibration curve for this oxidation process, indicating the relationship between current intensity (i) and glucose concentration (C) on a semilogarithmic plot. The calibration curve illustrates a wide linear range from 1.5 to 16 mM glucose (R^2 = 0.9958) with the regression equation $I(\mu A) = 12.78 \times C_{glucose}(mM) + 6.61$. This linear range overlaps the glucose concentration in healthy people (3-8 mM, 54-144 $mg.dL^{-1}$) [9, 26]. The limit of detection (LOD) estimated from the calibration curve for the sensor was 25 µM (S/N: 3), and the calculated sensitivity was 48.4 $\mu A.mM^{-1}.cm^{-2}$. The high achieved sensitivity and wide dynamic range in glucose detection could be attributed to the following two reasons: (1) the integration of the carbon-based working electrode and the dual porous gold electrocatalyst by electrodeposition eliminates the hetero-interface and contact resistance between them, leading to very fast electron transport, and (2) the interconnected electrolyte-filled dual porous network guarantees high accessibility and enables rapid mass transport [43].

Table 1. Comparison of preparation and features of enzyme-free glucose sensors at various porous electrodes.

Electrode	**Preparation time (h)**	**Linear range (mM)**	**LOD (µM)**	**Sensitivity ($\mu A.mM^{-1}.cm^{-2}$)**	**Ref**
Micro-nano dual porous gold	~ 0.08	1.5-16	25	48.4	This work
3D porous Au-gra	0.25	0.1–2.0	25	5.20	[41]
Porous gold cluster film	Not given	0.01 − 10	1	10.76	[42]
Gold nanoparticles modified glassy carbon	Up to 24	0.1 - 25	50	87.5	[44]
Gold micropillar array	~0.05	0.5-9	60	13.2	[26]
Porous gold film	~11	2-10	5	11.8	[34]
Gold porous (Amalgamation)	~ 0.02	2-20	2	32	[37]
Gold film electrode 3DGFE	~1.5	$5x10^{-3}$- 10	3.2	46.6	[23]
Gold nanocoral	~18	0.05-30	10	22.6	[45]
Self-assembled 3D gold nanoparticles	~18.5	0-8	0.005	179	[7]
Pt MWCNTs	~1	1-23	50	11.83	[46]

Pt nanoflowers	Not given	1-16	48	1.87	[47]
Ni foam	Not given	0.05-7.35	2.2	-	[43]
CuO porous	~5	0.001-2.5	0.14	2900	[25]
CuO MWCNTs	Not given	0.0004-1.2	0.2	2596	[48]

A comparison between the developed MNDP gold-modified SPCE and some other non-enzymatic glucose sensors based on porous materials is summarized in Table 1. As can be observed, the presented electrode displays better sensitivity for glucose detection when compared to the other electrodes, with the exception of the self-assembled 3D gold electrode [6] and two porous CuO-based electrodes [19, 36], which measured glucose oxidation in a high pH medium (pH = 9.2 for the self-assembled 3D gold electrode) and alkaline medium. High pH and alkaline medium are known to strongly support glucose oxidation and accelerate the catalytic abilities of gold and CuO. In addition, the obtained linear range and LOD are also compatible with those obtained with most other gold and platinum-based electrodes [26, 34, 37, 44-47], but the linear dynamic range is much better than that of CuO based electrodes [25, 48], which exhibited a dynamic range lower than normal physiological glucose levels (3-8 mM). Furthermore, the developed sensor presents advantages, such as small size, compact type and very short preparation time (0.08 h). This is a definite improvement compared with other electrodes, which are prepared with complicated processes, such as Hummer's method, chemical vapor deposition or using hazardous material such as mercury for amalgamation. The short preparation time and three-dimensional microstructure have high potential applications as enzyme-free glucose sensors.

3.4. Interference and detection of glucose in human serum

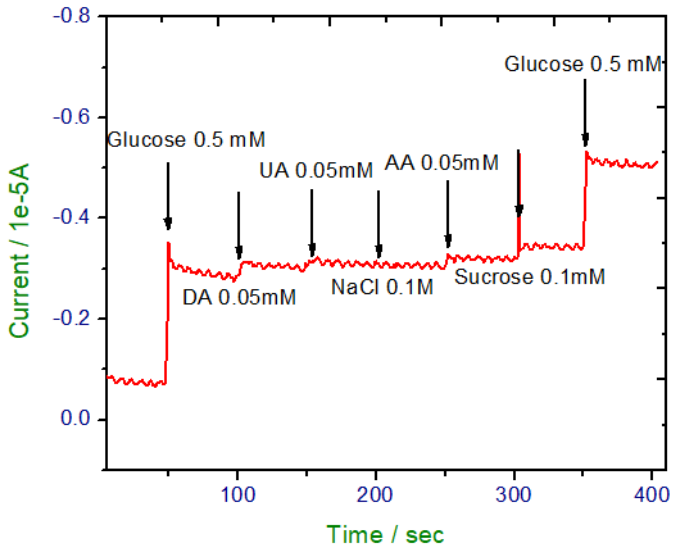

Figure 5. Amperometric response of the MNDP gold-modified SPCE upon successive addition of glucose (0.5 mM), interferences (0.05 mM DA, 0.05 mM UA, 0.1 M NaCl, 0.05 mM AA, and

0.1 mM sucrose) and then glucose (0.05 mM). The applied potential was -0.20 V vs. AgCl/Ag at a constant speed of 500 rpm.

As previously mentioned, elimination of the effects of easily oxidized compounds' co-existence in the biological sample during the glucose sensing process is a real challenge. Many substances co-exist in the biological fluid, such as dopamine (DA), uric acid (UA), ascorbic acid (AA), sucrose, saline, which interfere with agent in the real sample (blood or serum). These interferences must be removed to accurately measure glucose concentration [7]. Here, the selectivity for the present electrode for detecting glucose was studied in the presence of 0.05 mM DA, 0.05 mM UA, 0.1 M NaCl, 0.05 mM AA, and 0.1 mM sucrose, which are similar levels to those in normal physiological conditions [7, 9]. As shown in Figure 6, MNDP gold-modified SPCE exhibits negligible amperometric response to interference. This result is in good agreement with previous reports [19]. The combined presence of interfering substances in the sample does not affect the amperometric response of glucose.

Table 2. Comparison of the glucose sensor developed in this report and BT 3000 Plus (Biotecnica Instruments) to detect serum glucose concentration (n = 3).

Sample (human blood serum)	BT 3000 Plus (mM)	This glucose sensor (mM)	Spiked (mM)	Found (mM)	Recover (%)
#1	4.6	5.05 ± 0.17			
#2	5.7	5.37 ± 0.21			
#3	5.1	5.19 ± 0.09	2.00	7.39± 0.20	102.3%
			4.00	9.43± 0.18	102.6%

To verify the sensor's feasibility for practical analysis, the MNDP gold-modified SPCE was used to quantitatively detect glucose in human blood serum using the standard addition method. BT 3000 Plus (Biotecnica Instruments) was also used to analyze glucose levels in these samples for comparison, with results shown in Table 2. The obtained results are consistent with those detected by a biochemistry analyzer in clinical use. The deviation of the detected glucose concentration of the developed glucose sensor compared with that of the BT 3000 Plus was less than 9.7% (n=3). The results shown in Table 2 also indicate a recovery range approximately 102.3% (n=3) when glucose is spiked in the serum sample. This indicates that the developed sensor is highly accurate. Therefore, the glucose sensor developed in this report possesses promising potential to detect glucose concentrations in real samples.

4. CONCLUSION

The combination of MNDP gold with SPCE leads to a compact, simple assay system. The MNDP gold structure on SPCE was synthesized via a simple electrochemical deposition technique. MNDP gold-modified SPCE showed high catalytic efficiency for glucose oxidation in neutral pH

without support from enzymes or redox mediators. This enzyme-free glucose sensor exhibits high sensitivity, selective properties with a limit of detection as low as 25 µM and an extensive dynamic range from 25 µM to 16 mM. The sensor also shows the ability to detect glucose levels in real samples with good recovery (~103%). Our enzyme-free sensor would extend the clinical indices for glucose as indices for fitness not only to patients with diabetes but also to the general population.

ACKNOWLEDGEMENTS
This research is funded by the Vietnam National University, Hanoi (VNU) under project number QG.17.15.

References

1. A. Heller, B. Feldman, *Accounts of Chemical Research*, 43 (2010) 963.
2. A. Heller, B. Feldman, *Chemical Reviews*, 108 (2008) 2482.
3. H. Zhu, L. Li, W. Zhou, Z. Shao, X. Chen, *Journal of Materials Chemistry B*, 4 (2016) 7333.
4. Y. Bai, Y. Sun, C. Sun, *Biosensors and Bioelectronics*, 24 (2008) 579.
5. S. Park, H. Boo, T.D. Chung, *Analytica Chimica Acta*, 556 (2006) 46.
6. P. Si, X.-C. Dong, P. Chen, D.-H. Kim, *Journal of Materials Chemistry B*, 1 (2013) 110.
7. B.K. Jena, C.R. Raj, *Chemistry-A European Journal*, 12 (2006) 2702.
8. Y. Xia, W. Huang, J. Zheng, Z. Niu, Z. Li, *Biosensors and Bioelectronics*, 26 (2011) 3555.
9. K.E. Toghill, R.G. Compton, *Int J Electrochem Sci*, 5 (2010) 1246.
10. C. Su, C. Zhang, G. Lu, C. Ma, *Electroanalysis*, 22 (2010) 1901.
11. F. Xu, K. Cui, Y. Sun, C. Guo, Z. Liu, Y. Zhang, Y. Shi, Z. Li, *Talanta*, 82 (2010) 1845.
12. L.-M. Lu, H.-B. Li, F. Qu, X.-B. Zhang, G.-L. Shen, R.-Q. Yu, *Biosensors and Bioelectronics*, 26 (2011) 3500.
13. S. Li, Y. Zheng, G.W. Qin, Y. Ren, W. Pei, L. Zuo, *Talanta*, 85 (2011) 1260.
14. X. Zhang, A. Gu, G. Wang, Y. Wei, W. Wang, H. Wu, B. Fang, *CrystEngComm*, 12 (2010) 1120.
15. Y. Zhang, D. Zhao, W. Zhu, W. Zhang, Z. Yue, J. Wang, R. Wang, D. Zhang, J. Wang, G. Zhang, *Sensors and Actuators B: Chemical*, 255 (2018) 416.
16. H. Wu, Y. Yu, W. Gao, A. Gao, A.M. Qasim, F. Zhang, J. Wang, K. Ding, G. Wu, P.K. Chu, *Sensors and Actuators B: Chemical*, 251 (2017) 842.
17. Z. Qin, Q. Cheng, Y. Lu, J. Li, *Applied Physics A*, 123 (2017) 492.
18. W.-D. Zhang, J. Chen, L.-C. Jiang, Y.-X. Yu, J.-Q. Zhang, *Microchimica acta*, 168 (2010) 259.
19. L.Y. Chen, X.Y. Lang, T. Fujita, M.W. Chen, *Scripta Materialia*, 65 (2011) 17.
20. G.-X. Zhong, W.-X. Zhang, Y.-M. Sun, Y.-Q. Wei, Y. Lei, H.-P. Peng, A.-L. Liu, Y.-Z. Chen, X.-H. Lin, *Sensors and Actuators B: Chemical*, 212 (2015) 72.
21. J. He, W. Zhou, J. Sunarso, X. Xu, Y. Zhong, Z. Shao, X. Chen, H. Zhu, *Electrochimica Acta*, 260 (2018) 372.
22. J. Li, R. Yuan, Y. Chai, X. Che, W. Li, X. Zhong, *Microchimica Acta*, 172 (2011) 163.
23. Y. Bai, W. Yang, Y. Sun, C. Sun, *Sensors and Actuators B: Chemical*, 134 (2008) 471.
24. H.-C. Shin, M. Liu, *Chemistry of materials*, 16 (2004) 5460.
25. S. Cherevko, C.-H. Chung, *Talanta*, 80 (2010) 1371.
26. R. Prehn, M. Cortina-Puig, F.X. Muñoz, *Journal of The Electrochemical Society*, 159 (2012) F134.
27. M. Tominaga, T. Shimazoe, M. Nagashima, H. Kusuda, A. Kubo, Y. Kuwahara, I. Taniguchi, *Journal of Electroanalytical Chemistry*, 590 (2006) 37.
28. K. Idegami, M. Chikae, K. Kerman, N. Nagatani, T. Yuhi, T. Endo, E. Tamiya, *Electroanalysis*,

20 (2008) 14.
29. L.T. Truong, M. Chikae, Y. Ukita, Y. Takamura, *Talanta*, 85 (2011) 2576.
30. T. Truong, X.V. Nguyen, M. Chikae, Y. Ukita, Y. Takamura, *Journal of Biosensors and Bioelectronics*, 2 (2011) 1.
31. K. Charoenkitamorn, P. Tue, K. Kawai, O. Chailapakul, Y. Takamura, *Sensors*, 18 (2018) 444.
32. S. Cherevko, C.-H. Chung, *Electrochemistry Communications*, 13 (2011) 16.
33. N.X. Viet, Y. Takamura, *VNU Journal of Science: Natural Sciences and Technology*, 32 (2016) 83.
34. Y. Li, Y.-Y. Song, C. Yang, X.-H. Xia, *Electrochemistry Communications*, 9 (2007) 981.
35. Y. Ding, J. Erlebacher, *Journal of the American Chemical Society*, 125 (2003) 7772.
36. H. Qiu, C. Xu, X. Huang, Y. Ding, Y. Qu, P. Gao, *The Journal of Physical Chemistry C*, 112 (2008) 14781.
37. S. Cho, C. Kang, *Electroanalysis*, 19 (2007) 2315.
38. Y.Y. Song, D. Zhang, W. Gao, X.H. Xia, *Chemistry-A European Journal*, 11 (2005) 2177.
39. R. Adzic, M. Hsiao, E. Yeager, *Journal of electroanalytical chemistry and interfacial electrochemistry*, 260 (1989) 475.
40. L. A Larew, D.C. Johnson, *Journal of electroanalytical chemistry and interfacial electrochemistry*, 262 (1989) 167.
41. H. Shu, G. Chang, J. Su, L. Cao, Q. Huang, Y. Zhang, T. Xia, Y. He, *Sensors and Actuators B: Chemical*, 220 (2015) 331.
42. L. Han, S. Zhang, L. Han, D.-P. Yang, C. Hou, A. Liu, *Electrochimica acta*, 138 (2014) 109.
43. W. Lu, X. Qin, A.M. Asiri, A.O. Al-Youbi, X. Sun, *Analyst*, 138 (2013) 417.
44. G. Chang, H. Shu, K. Ji, M. Oyama, X. Liu, Y. He, *Applied Surface Science*, 288 (2014) 524.
45. T.-M. Cheng, T.-K. Huang, H.-K. Lin, S.-P. Tung, Y.-L. Chen, C.-Y. Lee, H.-T. Chiu, *ACS applied materials & interfaces*, 2 (2010) 2773.
46. L.-H. Li, W.-D. Zhang, *Microchimica Acta*, 163 (2008) 305.
47. M. Guo, H. Hong, X. Tang, H. Fang, X. Xu, *Electrochimica acta*, 63 (2012) 1.
48. L.-C. Jiang, W.-D. Zhang, *Biosensors and Bioelectronics*, 25 (2010) 1402.